1 **Enhanced Terrestrial Runoff during Oceanic Anoxic Event 2 on the North**
2 **Carolina Coastal Plain, USA**

3 Christopher M. Lowery[1], Jean M. Self-Trail[2], Craig D. Barrie[3]

4 [1]University of Texas Institute for Geophysics, Austin, TX, USA
5 [2]United States Geological Survey, Reston, VA, USA
6 [3]GeoMark Research, LTD, Houston, TX, USA

7 *Correspondence to*: Chris Lowery cmlowery@utexas.edu

8 **Abstract**

9   A global increase in the strength of the hydrologic cycle drove an increase in the flux of

10 terrigenous sediments into the ocean during the Cenomanian–Turonian Oceanic Anoxic Event 2 (OAE2)

11 and was an important mechanism driving nutrient enrichment and thus organic carbon burial. This global

12 change is primarily known from isotopic records, but global average data don't tell us anything about

13 changes at any particular location. Reconstructions of local terrigenous flux can help us understand the

14 role of regional shifts in precipitation in driving these global trends. The proto-North Atlantic basin was

15 one of the epicenters of enhanced organic carbon burial during OAE2, and so constraining terrigenous

16 flux is particularly important in this region; however, few local records exist. Here, we present two new

17 OAE2 records from the Atlantic Coastal Plain of North Carolina, USA, recognized with calcareous

18 nannoplankton biostratigraphy and organic carbon isotopes. We use carbon/nitrogen ratios to constrain

19 the relative contribution of marine and terrestrial organic matter; in both cores we find elevated

20 contribution from vascular plants beginning just before OAE2 and continuing through the event,

21 indicating a locally strengthened hydrologic cycle. Terrigenous flux decreased during the brief change in

22 carbon isotope values known as the Plenus carbon isotope excursion, and then increase and remain

23 elevated through the latter part of OAE2. TOC values reveal relatively low organic carbon burial in the

24 inner shelf, in contrast to black shales known from the open ocean. Organic carbon content on the shelf

25 appears to increase in the offshore direction, highlighting the need for cores from the middle and outer

26 shelf.

1

1 Introduction

The Cretaceous was characterized by intermittent periods of enhanced organic carbon burial linked to widespread black shale deposition and anoxia, termed Oceanic Anoxic Events (OAEs; Schlanger and Jenkyns, 1976; Jenkyns 2010). Although OAEs were originally defined by the widespread occurrence of black shales (Schlanger and Jenkyns, 1976) they were soon found to be associated with positive carbon isotope excursions driven by the excess global burial of organic carbon and representing a perturbation of the global carbon cycle (Scholle and Arthur, 1980; Arthur et al., 1987; Jenkyns, 2010; Owens et al., 2017). OAEs eventually became linked with the emplacement of large igneous provinces (Tarduno et al., 1991; Whitechurch et al., 1992; Leckie et al., 2002; Snow et al., 2005; Turgeon and Creaser, 2008; Monteiro et al., 2012; McAnena et al., 2013), suggesting a causal mechanism for enhanced organic carbon burial. In the case of the Cenomanian–Turonian OAE2 ($\sim$ 94 Ma), the emplacement of the Caribbean Large Igneous Province (e.g., Snow et al.,2005) is associated with significant warming (e.g., Friedrich et al., 2012) and resulted in a strengthening of the hydrological cycle and an increase in the flux of nutrients to the oceans (Blättler et al., 2011; Pogge von Strandmann et al., 2013).

Carbon isotopes reveal global changes in organic carbon burial rates but don't tell us anything about where that organic matter was buried. This is important because local organic matter enrichment can vary significantly in both timing (e.g., Tsikos et al., 2004) and magnitude (e.g., Owens et al., 2018) during an OAE. Similarly, the calcium isotope proxy used by Blättler et al. (2011) and the lithium isotope proxy used by Pogge von Strandmann et al. (2013) to determine changes in global terrigenous flux to the oceans don't tell us anything about local patterns of terrigenous runoff. Presumably, like organic carbon burial, the hydrologic cycle did not increase uniformly, but instead some regions experienced a greater change than others. Unfortunately, few local records of changes in the hydrologic cycle during OAE2 have been documented. Van Helmond et al. (2014) used palynological and biomarker data from the Bass River core (Ocean Drilling Program Site 174X) on the coastal plain of New Jersey, USA, to document local warming associated with enhanced contribution of terrestrial organic matter during OAE2. While

52 this result clearly indicates a stronger hydrologic cycle during OAE2, it only represents a single locality.

53 Similar work from Wunstorf, Germany, in the Lower Saxony Basin, reveals a clear association between

54 terrigenous flux (measured by palynology and biomarker data) and black shale development, but this

55 association isn't limited to OAE2, with additional intervals of elevated terrigenous input and black shale

56 deposition continuing after the end of the carbon isotope excursion (van Helmond et al., 2015). In the

57 Western Interior Seaway of North America, increases in kaolinite (a clay mineral formed in humid

58 environments) during OAE2 may be the result of wetter conditions, but these trends may also be caused

59 by shifting sediment source areas (Leckie et al., 1998). Overall, these existing records paint an incomplete

60 picture.

61   To fully understand these trends, it is essential to develop similar datasets from additional

62 localities. Such work will allow a more geographically complete understanding of changes in

63 precipitation during OAE2 and thus provide a window into the mechanisms which drove hydroclimate

64 during the hottest part of the Cretaceous greenhouse. Here, we present two new OAE2 sections from

65 cores drilled by the United States Geological Survey (USGS) on the coastal plain of North Carolina, on

66 the Atlantic margin of North America (Figure 1). We use organic carbon isotopes and calcareous

67 nannoplankton biostratigraphy to identify the OAE2 interval and organic carbon/nitrogen (C/N) molar

68 ratios to detect changes in terrigenous flux. These cores are only the second and third OAE2 intervals

69 described on the Atlantic Coastal Plain after the Bass River core (Bowman and Bralower, 2005; van

70 Helmond et al., 2014) and thus also provide important context for the response of the inner shelf to

71 OAE2, filling in an important gap in an important region (e.g., Owens et al., 2018) during this well-
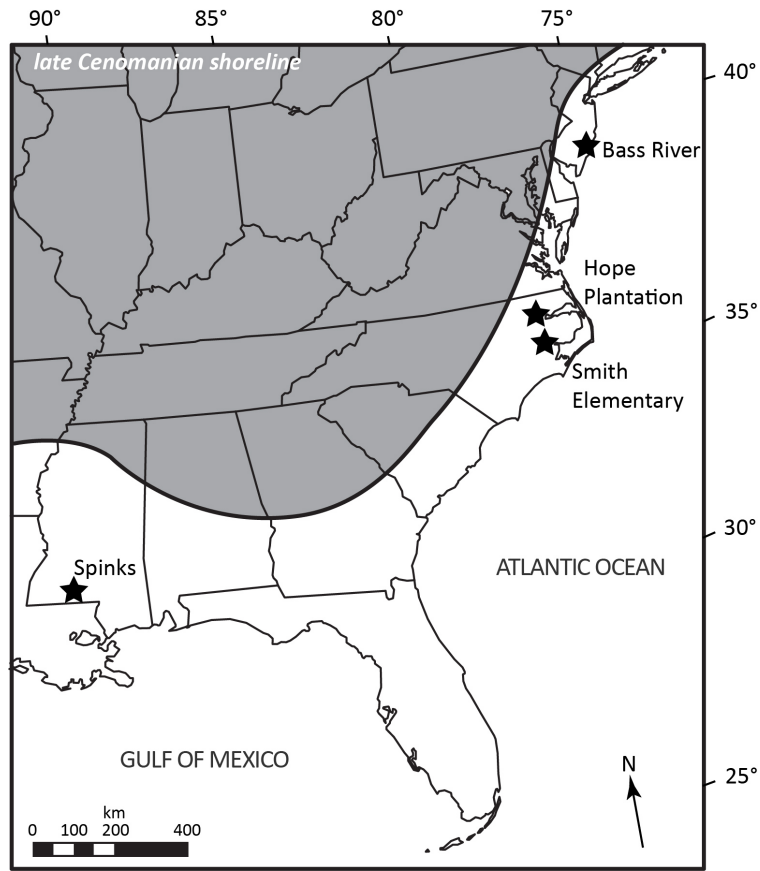
72 studied time interval.

Figure 1. *Map of southeastern North America showing approximate late Cenomanian shoreline (land = grey) and the location of the cores discussed in this study. Shoreline position after Slattery et al. (2015) and Snedden et al. (2015).*

2 Geologic Setting

Cenomanian and Turonian sediments of the Atlantic Coastal Plain of the United States (Figure 1) are part of a sequence of strata that accumulated since the rifting of the Atlantic began in the Early Jurassic. However, study of the marine units in these sediments is difficult due to the absence of outcrops of this age and environment and their moderate to large burial depths in the Carolinas and Georgia (Sohl and Owens, 1991). Thus, their study is restricted to the limited number of available cores and/or cuttings, and their regional interpretations are often based on geophysical data obtained from water wells and scattered oil and gas test wells.

85   To the south, initial subsurface work in Florida and Georgia followed the nomenclature of the

86   Gulf Coastal Plain. Sediments in Georgia were variously attributed to the Cenomanian Woodbine

87   Formation, the Cenomanian/Turonian Eagle Ford Formation, and the Cenomanian/Turonian Tuscaloosa

88   Formation (Applin and Applin, 1944; Richards, 1945). Applin and Applin (1947) later introduced the

89   name Atkinson Formation, with three unnamed members (upper, middle, and lower) for certain marine

90   and non-marine sediments in the subsurface of southern Alabama, southern Georgia, and northern

91   Florida. They correlated the lower member of the Atkinson to basal nonmarine sands and shales of the

92   coastal plain of Georgia, which they considered to be Cenomanian in age, and the middle member of the

93   Atkinson to the Tuscaloosa Marine Shale, which they considered to be Cenomanian/Turonian in age

94   (Applin and Applin, 1967).

95   Early work in South Carolina by Cooke (1936), Dorf (1952), and Heron (1958) considered

96   outcrops of the Middendorf Formation to be Cenomanian in age, based largely on stratigraphic position

97   and on long-ranging pollen and/or mollusks. Similarly, outcrops of the largely non-marine Cape Fear

98   Formation in North Carolina were attributed to the Cenomanian (Stephenson, 1912; Cooke, 1936).

99   Outcrops thought to be Turonian in age from both states were largely assigned to the Black Creek

100   Formation.

101   A shift in thinking regarding stratigraphic nomenclature was spurred by examination of sediments

102   from the Clubhouse Crossroads #1 core by Hazel et al. (1977), who found clear evidence of true

103   Cenomanian/Turonian marine sediments in the later-defined Clubhouse Formation near the base of the

104   downdip Coastal Plain section. Calcareous nannofossils and foraminifera of Cenomanian and Turonian

105   age were identified in the Clubhouse Formation (Hazel et al., 1977; Hattner and Wise, 1980; Valentine,

106   1984) and correlated with cuttings containing calcareous nannofossils from the Fripp Island, SC

107   deepwater well (Valentine, 1984). In North Carolina, Zarra (1989) reinterpreted the work of Spangler

108   (1950) using both foraminifera and sequence stratigraphic concepts, positively identifying Cenomanian

109   and Turonian sediments from the Esso #1 core and from cuttings of the Mobile #1, Mobile #2, Mobile #3,

110 and Marshall Collins #1 test wells. He used sediment and well log analysis to identify marginal marine

111 and inner shelf facies in the lower/middle Cenomanian and middle Turonian section, with a highstand in

112 the upper Cenomanian. These cores all contained a diverse assemblage of planktic foraminifera, including

113 species belonging to *Rotalipora, Praeglobotruncana, Dicarinella, Whiteinella,* and *Guembelitria* (Zarra,

114 1989).

115   This reevaluation ultimately resulted in the formal designation of the Cenomanian/Turonian

116 Clubhouse Formation (Gohn, 1992) in the Clubhouse Crossroads core. At the type locality, the Clubhouse

117 Formation consists of gray to gray-green, fine- to medium- grained, micaceous, muddy sands with flaser

118 to lenticular bedding and common bioturbation. Sequence stratigraphic analysis suggests that deposition

119 occurred in a shelf environment proximal to the shoreline and that these sediments represent latest

120 Cenomanian/earliest Turonian sea level rise prior to the early Turonian highstand event (Aleman

121 Gonzalez et al., 2020). The subsurface extent of this formation has now been documented across much of

122 South Carolina and North Carolina (Weems et al. 2007; Weems et al., 2019; Aleman Gonzalez et al.,

123 2020).

124   To the north, published documentation of marine Cenomanian/Turonian sediments from the mid-

125 Atlantic region appears to be limited to the E.G. Taylor No. 1-G well on the eastern shore of Virginia.

126 Valentine (1984) reports the presence of *Rotalipora greenhornensis,* which went extinct in the latest

127 Cenomanian, from one sample at 1520 ft.

128   Cenomanian/Turonian sediments of the northeast Atlantic Coastal Plain consist of the subsurface

129 Bass River Formation and its correlative updip equivalent, the Raritan Formation in Maryland, New

130 Jersey, and Delaware. The Bass River Formation is herein considered to be correlative with the

131 Clubhouse Formation of the southeastern Atlantic Coastal Plain. The Bass River Formation was first

132 described by Petters (1976) from the TC16 well in Bass River Township, New Jersey. It is considered to

133 be the fully marine equivalent of the Raritan Formation and is differentiated by its common shell material

134 and deeper water depositional environment (Miller et al., 1998). The Bass River Formation has variously

been assigned a late Cenomanian to early Turonian age in a variety of cores and wells based on

foraminifera (Petters, 1976, 1977; Miller et al., 1998; Sikora and Olsson, 1991), calcareous nannofossils

(Valentine, 1984; Miller et al., 1998; Self-Trail and Bybell, 1995), and ostracodes (Gohn, 1995). Miller

et al., (2004) document that the Bass River Formation was deposited predominantly in inner neritic to

middle neritic paleodepths.

3 Methods

3.1 Study Sites

The Hope Plantation core (BE-110-2004) was drilled by the USGS in April to May, 2004 in

Bertie County, North Carolina, on the property of Hope Plantation (36.0323°N; 78.0192°W) (Figure 1).

The hole was drilled as a stratigraphic test for Atlantic Coastal Plain aquifers, and was continuously cored

to a total depth of 333.6 m (1094.5 ft) below land surface. A suite of wireline logs, including natural

gamma ray and resistivity logs, were collected at the completion of drilling. Preliminary biostratigraphy

placed the marine Cenomanian/Turonian boundary interval between approximately 182.8-228.6 m (600-

750 ft). A summary of the general stratigraphy, downhole logging, and core images can be found in

Weems et al. (2007).

The Smith Elementary School core (CR-675) was drilled by the USGS in February and March,

2006 in Craven County, NC, on the grounds of the nominate school (35.2511°N; 77.2903°W) (Figure 1).

This hole was also drilled as a stratigraphic test for coastal plain aquifers, and was continuously cored to a

total depth of 323.1 m (1094.5 ft). Difficulties with the wireline tools and borehole stability limited the

collection of geophysical logs, and only a partial natural gamma ray log exists for the Clubhouse

Formation in this corehole. There, the marine interval that spans the Cenomanian/Turonian boundary is

between 288.3 and 323.1 m depth (945.9-1060.0 ft). Both cores are stored at the North Carolina

Geological Survey Coastal Plain core storage facility in Raleigh, NC, where we sampled them in May,

2019.

159   **3.2 Calcareous Nannofossils**

160   One hundred and ten samples from Hope Plantation and 84 samples from Smith Elementary

161   School were examined for calcareous nannofossil content. Samples were taken from the central portion of

162   broken core in order to avoid contamination from drilling fluid. Smear slides were prepared using the

163   standard techniques of Bown and Young (1998) in samples with low total organic carbon (TOC); samples

164   with increased TOC were prepared using the techniques of Shamrock et al. (2015) and Shamrock and

165   Self-Trail (2016). Coverslips were affixed using Norland Optical Adhesive 61. Calcareous nannofossils

166   were examined using a Zeiss Axioplan 2 transmitted light microscope at 1250x magnification under

167   crossed polarized light. Light microscope images were taken using a Powershot G4 camera with a Zeiss

168   phototube adaptor. Specimens were identified to the species level and correlated to the zonation schemes

169   of Sissinghi (1977) and Burnett (1998), as modified by Corbett et al. (2014) for shelf settings.

170   **3.3 Foraminifera**

171   Ninety samples were prepared for examination of planktic and benthic foraminifera.

172   Approximately 15 grams of material were soaked in a mixture of peroxide and borax for at least 24 hours,

173   washed over a 63 μm sieve, dried overnight in an oven, and then examined for microfossils using a Zeiss

174   Discovery V8 light microscope.

175   **3.4 TOC, C/N, and δ^{13}C**

176   Core samples were analyzed for both their elemental composition (%C and %N) and organic

177   carbon isotope signature (δ^{13}C VPDB). To remove inorganic carbon content all of the material to be

178   analyzed was initially washed with 1M hydrochloric (HCl) acid. There was no anticipated inorganic

179   nitrogen content in the samples. All of the samples were analyzed on an elementar vario ISOTOPE select

180   cube elemental analyzer (EA) connected to a VisION isotope ratio mass spectrometer (IRMS). The EA

181   system follows dumas combustion and both generates and separates the gasses used for elemental

182   composition determination and then releases the gas to the IRMS for isotopic determination. Every fifth

183   sample was run in duplicate and a check standard was run in triplicate every twentieth sample to ensure

184   the accuracy of the results. The elemental results were calibrated against a known sulfanilamide standard

185   and the precision of the results is +/-0.1% or better, and variation of duplicate samples was within range

186   of this uncertainty. The carbon isotope results were calibrated against four known reference standards

187   which cover the range of isotopic signatures expected in organic material (-15‰ to -35‰), and duplicates

188   and check standards were run at the same interval as above. All of the isotopic results are reported in per

189   mil (‰) relative to VPDB and the precision of the results is +/-0.1‰ or better.

190   **4 Results**

191   **4.1 Lithology**

192   Qualitative core descriptions are summarized below and in Figures 2 and 3. Broad

193   paleoenvironmental interpretations are based on lithology, paleontology, and stratigraphic relationships.

194   Benthic foraminifera, which are powerful tools to determine paleoenvironment in marginal marine

195   settings (e.g., Tibert and Leckie, 2004), are unfortunately absent here due to poor preservation (see

196   section 4.2 below). In both cores we recognize two informal members of the Clubhouse Formation: a

197   marine lower member characterized by bivalves, calcareous nannoplankton, finer grained sediments,

198   thinner beds, and sedimentary features common to inner neritic environments; and a marginal marine

199   upper member characterized by coarser grainsize, thicker beds, and woody plant debris instead of

200   calcareous marine fossils, indicating deposition in a delta front or distributary environment.
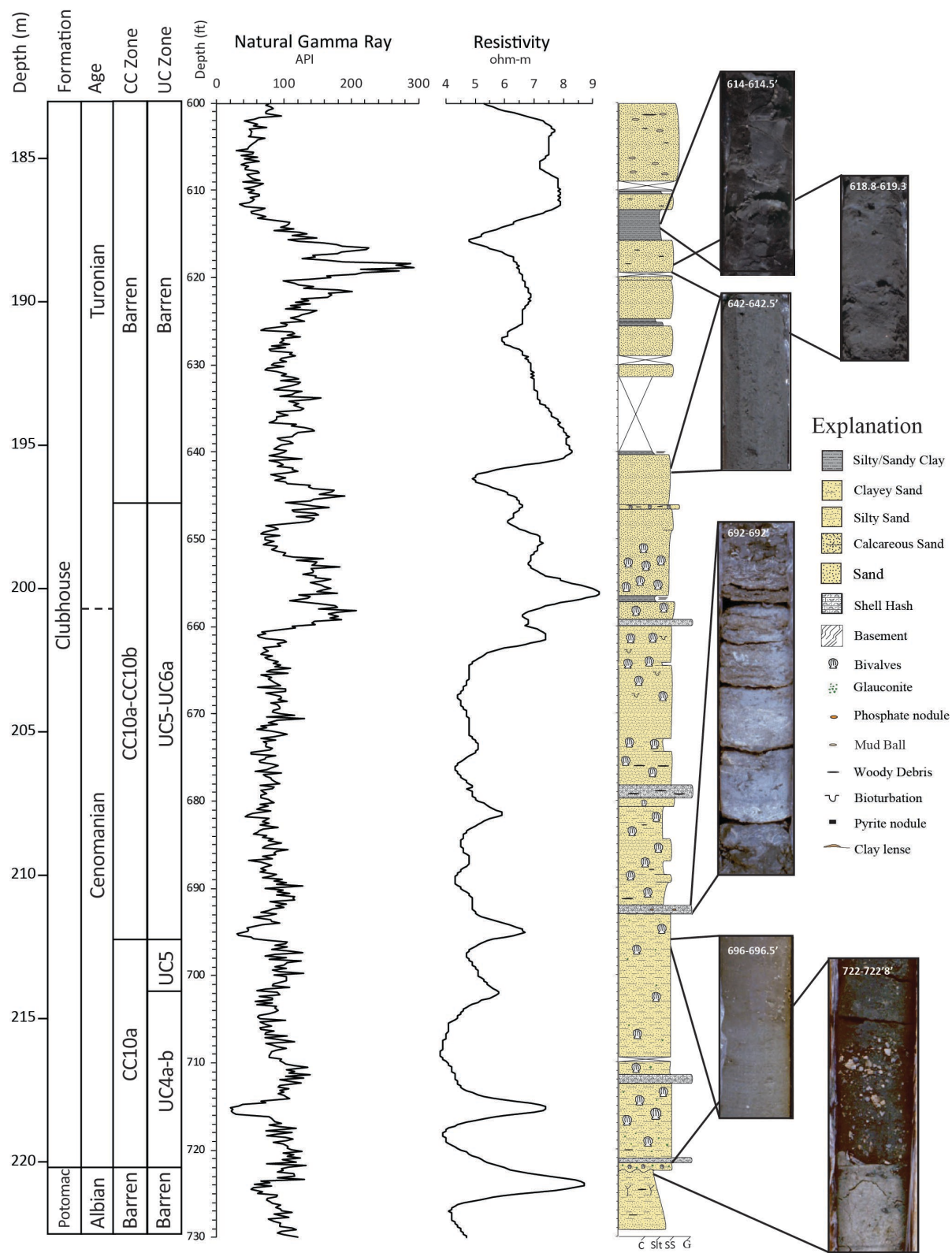
Figure 2. *Stratigraphic column for Hope Plantation Core with CC and UC calcareous nannoplankton biozones, natural gamma ray and resistivity logs, and representative core images. C = clay; Slt = silt; SS = sand; G = gravel.*

202   The Clubhouse Formation in the Hope Plantation Core (Figure 2) was penetrated between 174.3

203   m and 220.2 m below the surface. It is underlain by the floodplain paleosols of the Albian Potomac Group

204   (Thornburg, 2008) and is overlain by undifferentiated sands and muds questionably assigned to the Cape

205   Fear Formation (Weems et al., 2007). The Clubhouse Formation is primarily composed of clayey and

206   silty sands punctuated by a few discrete skeletal limestones. The whole unit coarsens upward from clayey

207   sands (from the base of the formation to about 210.0 m) to silty sands (from about 210.0 m to about 201.2

208   m) to more pure sands (from about 201.2 m to the top of the formation, although natural gamma ray peaks

209   suggest the inclusion of some clay in parts of this interval). This upper change corresponds with a clear

210   change in gamma ray log response that characterizes most of the informal marginal marine upper

211   member.

212   The lower marine informal member extends from the base of the Clubhouse Formation to the

213   highest common occurrence of bivalves and calcareous nannoplankton, around 196.9 m. Glauconite

214   occurs from the base of the informal marine unit up to about 211.2 m. Four decimeter-scale skeletal

215   limestones composed of broken bivalves occur roughly evenly spaced through this informal member.

216   Widely scattered woody debris is found between 210.6 m and 206.0 m. Definite bioturbation is rare but is

217   evident between 203.6 and 201.2 m, just below the shift in lithology from silty sand to cleaner sand.

218   Bivalves occur throughout the informal marine member in varying abundance. The marginal marine

219   upper informal member of the Clubhouse Formation is characterized by massive sand interbedded with

220   variably thick beds of massive silty clay, an increasing abundance of woody debris above 189.0 m, and

221   the occurrence of cm-scale mud balls above 185.6 m. A single thin bed containing bivalves occurs at

222   196.9 m. Given the more terrestrial features, cleaner sands, and thin clay interbeds of the upper informal

223   member of the Clubhouse Formation we suggest that these sediments were deposited in a non-marine or

224   marginal marine environment such as a distributary mouth bar or interdistributary bay system in the upper
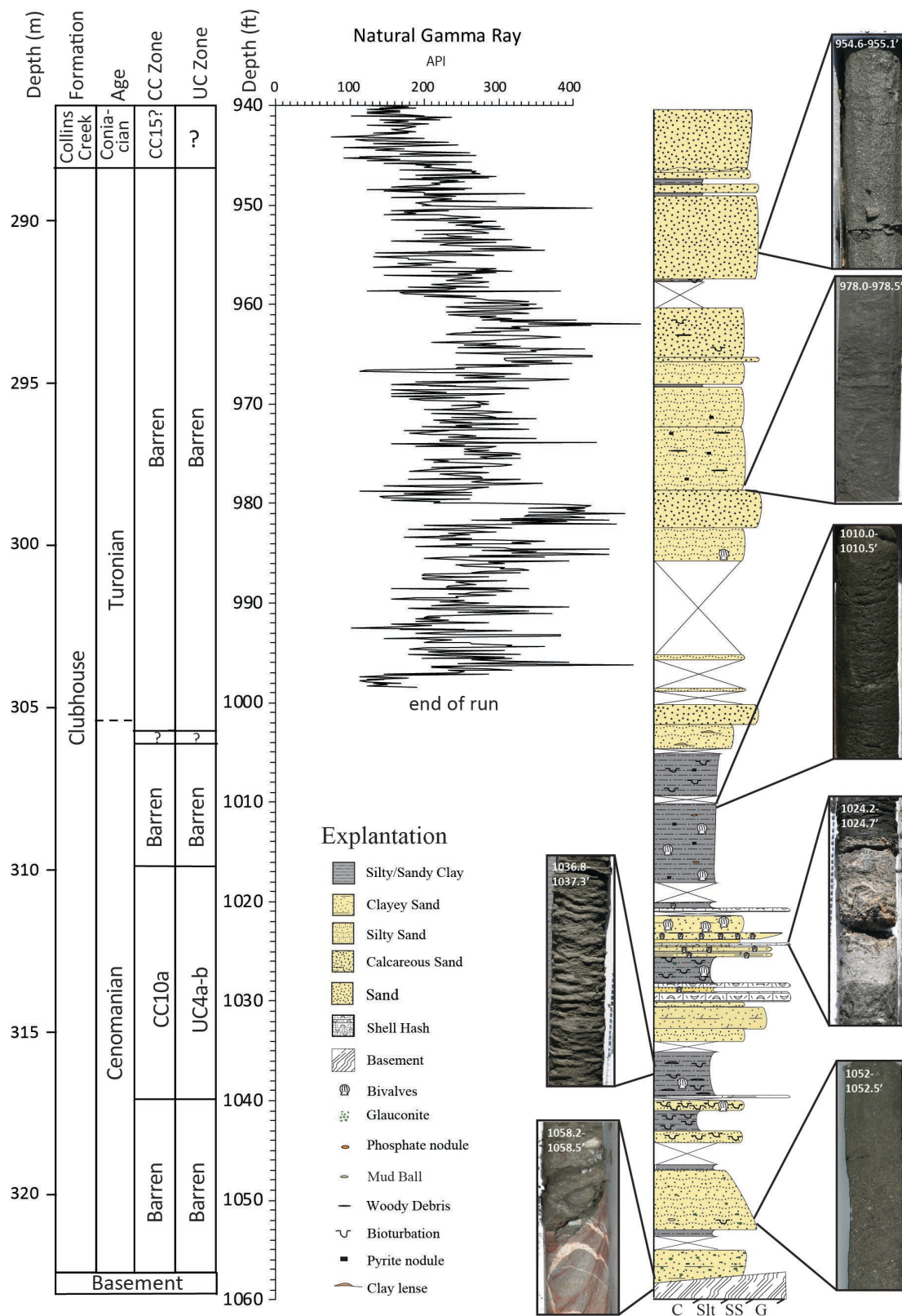
225   part of the Clubhouse Formation.

Figure 3. Stratigraphic column for the Smith Elementary School core, with CC and UC calcareous nannoplankton biozones, natural gamma ray log, and representative core images.

227   In the Smith Elementary core (Figure 3), the Clubhouse Formation occurs between 288.5 m and

228   322.7 m depth. Its basal contact with underlying gneiss is marked by a fault, with an angular contact

229   (~45° to vertical in the core) and slickensides (Weems et al., 2007). This fault is overlain by ~15 cm thick

230   interval of dolomitic sand. The lithology of the Clubhouse Formation in the Smith Elementary core is

231   overall more fine-grained than that of the Hope Plantation, with a lower fining-upwards interval, muds

232   and limestones in the middle, and a coarsening upward interval that extends to the unconformable upper

233   contact with the Santonian marginal marine Collins Creek Formation.

234   The lower marine informal member of the Clubhouse Formation in the Smith Elementary core

235   (322.7-~305.0 m) contains a more varied lithology than that of the Hope Plantation core. The basal

236   interval in this member is a 2.6 m thick package of massive, coarsening upward and then fining upward,

237   clayey to silty, glauconite-bearing sandstone separated by a thin silty claystone above a ~35 cm core gap.

238   Coring gaps of this scale are more common in the Smith Elementary core and are associated with the

239   contacts between sand and clay intervals. A single burrow occurs in the upper sandstone bed, and

240   glauconite decreases upsection. The overlying interval is composed of 2.8 m of bioturbated clay and silty

241   clay, with two ~30 cm thick silty sandstones with abundant burrows and rare bivalves. The upper silty

242   claystone contains thin clay lenses. This claystone is overlain by a 4.0 m thick interval of interbedded

243   silty- to clayey sandstone, skeletal limestones composed of broken bivalve debris, including one which

244   has been dolomitized, and a thick (~ 80 cm) bioturbated silty claystone containing glauconite and bivalve

245   shells. This in turn is overlain by a 5.2 m thick silty claystone with planar bedding, phosphate nodules,

246   pyrite, and bivalve shells. The lower 3.4 m of this claystone is laminated with no visible bioturbation.

247   Overall this interval represents a fining upward sequence from sand to sandy silt to silty clay; the sandy

248   clay contains thin discrete beds of coarser material, include shell hash, possibly indicating deposition

249   above storm wave base before deepening to uniform silty clay representing deposition on the shelf below

250   storm wave base at the top of the informal marine member.

251   The upper marginal marine informal member of the Clubhouse Formation in the Smith

252   Elementary core (~305.0-288.5 m) is composed of meter-scale beds of silty to well-sorted sandstone

253   which generally become coarser up section, interbedded with centimeter scale beds of claystone. Some

254   beds contain woody debris and pyrite. A single bivalve occurs near the very base of the member, and a

255   few discrete burrows are observed between 294 and 292 m. Flaser bedding occurs in a clay bed at 291.7

256   m. The overall coarse-grained nature of these beds, and the alternating terrestrial and marine indicators

257   lead us to interpret this interval as being marginal marine, perhaps representing distributary mouth bars.

258   The overlying contact with the Collins Creek Formation is marked by a readily observable unconformity.

259   **4.2 Biostratigraphy**

260   Calcareous nannofossil assemblages are prevalent in the Hope Plantation core (Figure 4), with

261   abundances ranging from rare to common and preservation from good to poor; the top of the Clubhouse

262   Formation is barren (196.8-185.5 m) (Self-Trail et al., 2021). The base of the Clubhouse Formation is

263   placed in the late Cenomanian Zone UC4a-b of Burnett (1998) and Zone CC10a of Sissinghi (1977)

264   based on the presence *of Lithraphidites acutus*, whose highest occurrence (HO) at 214.0 m marks the top

265   of Zone UC4b. The absence of *Cretarhabdus loriei*, whose HO marks the top of UC4a, could be due to

266   ecological exclusion from inshore environments, and thus sediments in this interval are lumped together

267   into a combined zone (UC4a-b). A condensed (or truncated) interval from the HO of *L. acutus* to the HO

268   of *Helenea chiastia* at 212.9 m is placed in Zone UC5 (undifferentiated) and is latest Cenomanian in age.

269   It is unclear from nannoplankton data alone whether the HO of *H. chiastia* is the true extinction of this

270   taxon (and thus this level marks the latest Cenomanian) or if this absence of this species above the level is

271   the result of poor preservation and/or ecological exclusion from the inner shelf as increased terrigenous

272   flux made the waters less welcoming to marine nannoplankton. We favor the latter explanation, because

273   the sample immediately above the highest *H. chiastia* is barren, and marks the beginning of an interval

274   characterized by poor preservation and locally barren samples. This interval, from 212.1-197.0 m, is

275   placed in zones UC5-UC6a and CC10a-CC10b based on the absence of both *H. chiastia* and *Eprolithus*

276 *moratus*, whose lowest occurrence (LO) defines the base of Zone UC6b. The Cenomanian/Turonian

277 boundary is placed at 200.3 m based on carbon isotope data (see section 4.3.1, below).
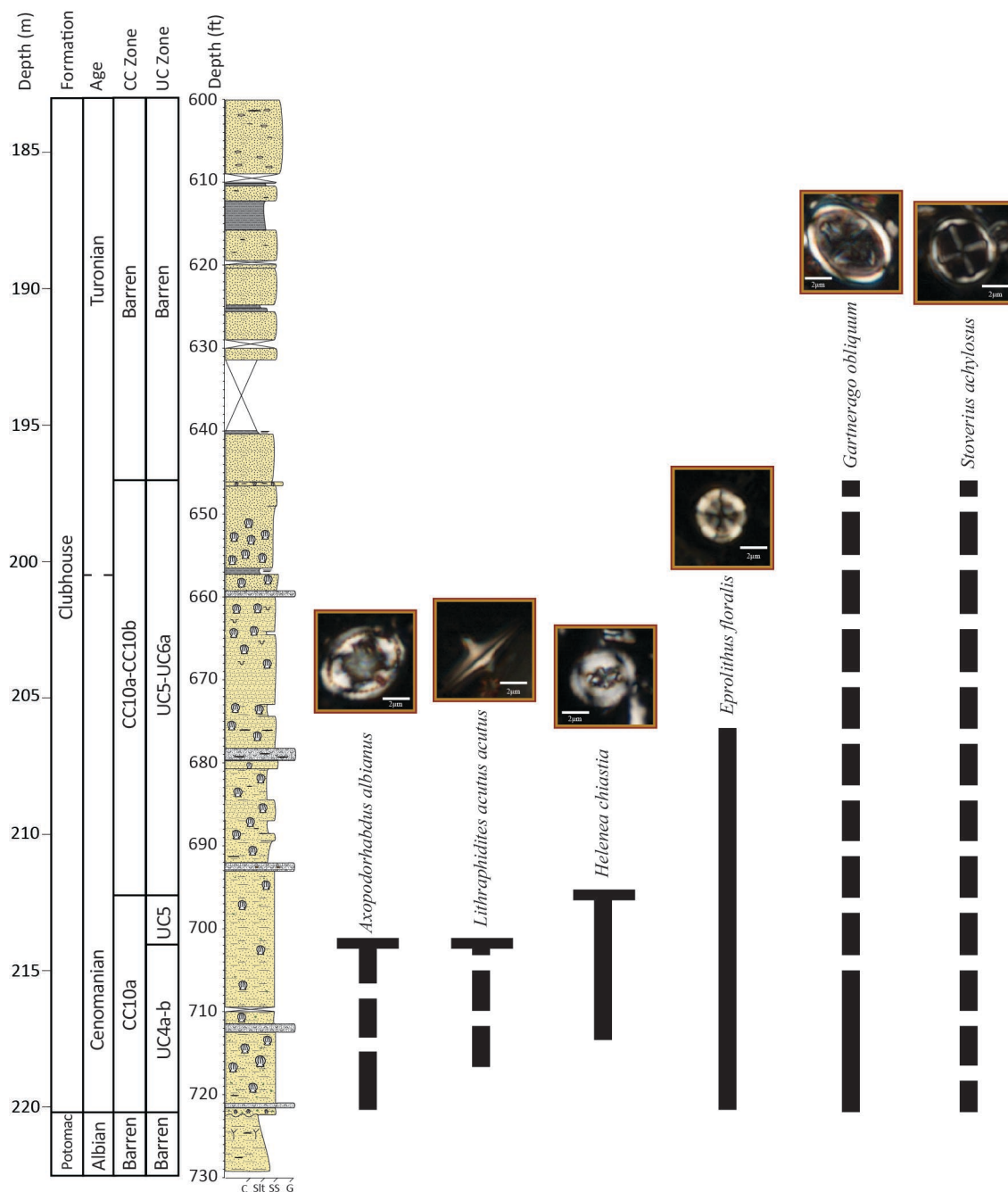
278

279 ***Figure 4.*** *Ranges of key calcareous nannoplankton species in the Hope Plantation Core. Dashed lines indicate*
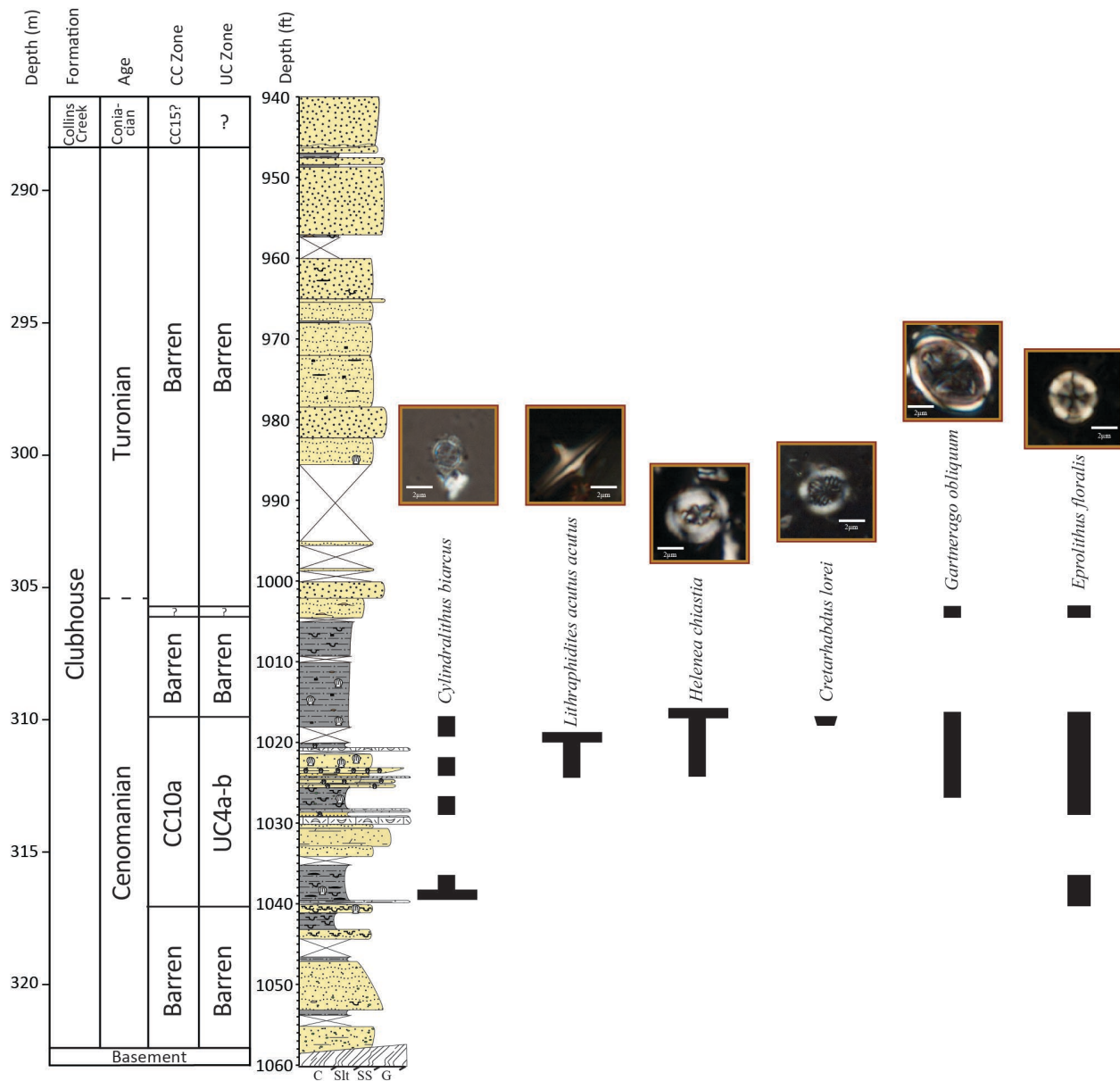280 *sporadic occurrence.*

Figure 5. *Ranges of key calcareous nannoplankton species in the Smith Elementary School core. Dashed lines indicate sporadic occurrences.*

Calcareous microfossils are only sporadically present in the Smith Elementary School sediments (Self-Trail et al., 2021) (Figure 5). Even though the presence of glauconite, burrowing, fish debris and scattered shell fragments indicates deposition in a marine environment, intervals barren of calcareous nannoplankton are common and extensive, from 322.5-317.3 m and 309.9-290.4 m (Figure 5). The presence of *Cylindralithus biarcus* at 316.4 m, the HO of *L. acutus* at 310.9 m, and the HOs of *H. chiastia*

289 and *C. loriei* at 310.2 m place this interval in the late Cenomanian calcareous nannofossil Zone UC4a-

290 b/Zone CC10a. The rare occurrence of poorly preserved calcareous nannofossils at 305.9 m suggests

291 continued placement in the Cenomanian or Turonian, but no diagnostic species were recovered, and thus

292 the Cenomanian/Turonian boundary must once again be placed using carbon isotopes at 305.4 m (see

293 section 4.3.1, below). An unconformity at the top of the Clubhouse Formation (288.4 m) corresponds to a

294 change from a barren interval below to a Santonian assemblage of calcareous nannofossils above.

295   All samples examined for planktic and benthic foraminifera were barren of whole specimens.

296 This is unlikely to be the result of anoxia at the time of deposition, as this would not explain the lack of

297 planktic foraminifera which occupied a mixed layer habitat similar to the nannoplankton observed in the

298 same interval. A few samples contained very rare fragments of both planktic and benthic foraminifera,

299 indicating that foraminifera were present in these sections but that they were subsequently dissolved,

300 either in situ or in the 17 years since the cores were drilled. This may be due in part to the relatively

301 organic-rich nature of the sediments and to the presence of pyrite, both of which have been found to result

302 in dissolution of calcareous microfossils in cored sediments of the Atlantic Coastal Plain (Self-Trail and

303 Seefelt, 2005; Seefelt et al., 2015). However, the well-documented occurrence of planktic and benthic

304 foraminifera in more distal coastal plain cores (e.g., Valentine, 1982, 1984; Zarra, 1989; Gohn, 1992)

305 bodes well for future micropaleontological studies in this region.

306 **4.3 Geochemistry**

307 **4.3.1 Carbon Isotopes**

308   Organic carbon isotope (δ^{13}C) data (Figure 6) in each core show clear positive excursions

309 associated with OAE2 in the marine interval of the Clubhouse Formation. Both isotope records display a

310 ~2‰ positive shift with the classic A-B-C structure of OAE2, with an initial excursion (A), a brief

311 recovery followed by a second peak (B) and a longer plateau with a small peak (C) first described by Pratt

312 and Threlkeld (1984) in the US Western Interior Seaway. The Hope Plantation core, which is

313 characterized by coarser grains and a more proximal environment, has a more expanded OAE2 interval (~

314 17.4 m) compared to the somewhat more distal Smith Elementary Core (~ 10.4 m). We compare the

315 expanded Hope Plantation carbon isotope record to other representative North American OAE2 records

316 from the Western Interior Sea and the Gulf of Mexico and Atlantic coastal plains in Figure 7. The

317 termination of the OAE2 carbon isotope excursion roughly corresponds with the Cenomanian–Turonian

318 boundary (e.g., Kennedy et al., 2005) and has been used to define that level in our cores.

319 **4.3.2 Total Organic Carbon**

320   Total organic carbon data (Figure 6) reveals relatively low enrichment in organic carbon in the

321 Hope Plantation core, generally <1 weight percent (wt%) TOC except for a few discrete peaks associated

322 with woody debris. Average values are slightly higher during OAE2 (~0.6 wt%) compared to background

323 levels in the overlying interval (~0.4 wt%) but just barely. Values are slightly higher overall in the Smith

324 Elementary School core, particularly during OAE2, where the upper part of the event averages about 1.0

325 wt% TOC.

326 **4.3.3 Organic Carbon/Nitrogen Ratios**

327   The ratio of total organic carbon to total nitrogen is a common proxy for the relative contributions

328 of algae and land plants to sedimentary organic matter (e.g., Meyers, 1994, 1997, 2003). Due to

329 differences in their composition (e.g., the abundance of cellulose in land plants) vascular plants tend to

330 have C/N ratios of 20 or greater, while algae have C/N ratios of 4-10 (Meyers, 1994). Changes in C/N

331 ratio in marine settings therefore reflect changes in the relative contribution of terrigenous organic matter

332 to offshore areas. C/N can thus be used to reconstruct changes in the hydrologic cycle, with increased C/N

333 ratios indicating a higher flux of terrestrial organic matter due to enhanced weathering (Meyers, 2003).

334 Sediments with low TOC (<0.3 wt%) can cause problems for C/N interpretations because in such settings

335 the proportion of inorganic nitrogen can be high enough to artificially depress the data, suggesting more

336 marine organic matter than is really there (Meyers, 1997); our data is consistently above 0.5 wt% TOC so

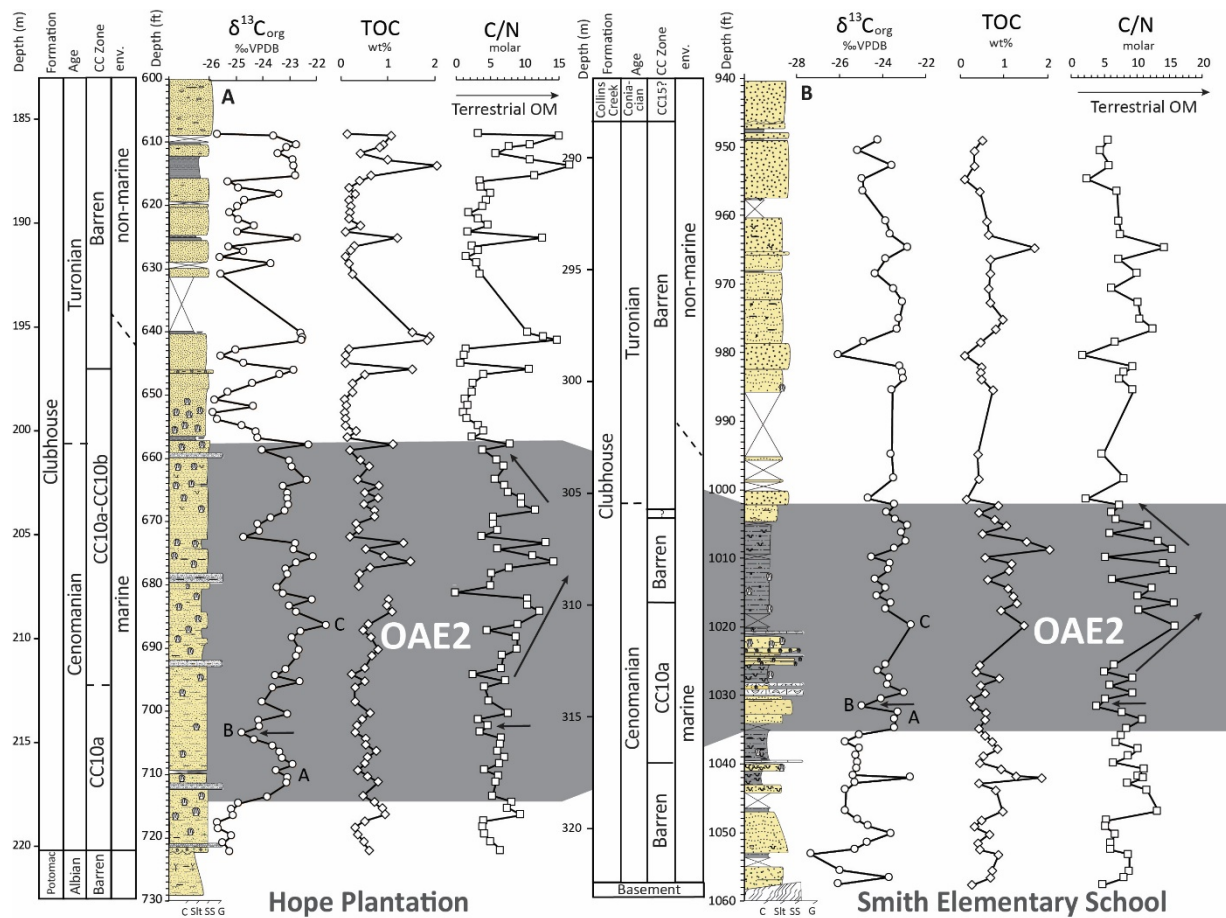337   this is not a concern (see section 4.3.2, above).

Figure 6. Geochemical data from the Hope Plantation (left) and Smith Elementary School (right) cores plotted against stratigraphic columns for each. Grey shaded area represents the OAE2 interval in each core. Letters A-B-C labels on carbon isotope (δ13C) curve correspond to named points of the OAE carbon isotope excursion. TOC = total organic carbon; C/N = carbon/nitrogen ratio. Arrows indicate brief reduction in C/N ratio coincident with the Plenus isotope excursion ("B" on the δ13C plot) and broad increase in values during the main part of the δ13C excursion. Note slight change in depth scale between the two cores, as the studied interval in Smith Elementary is 10 ft (3.1 m) thicker than Hope Plantation.

346   C/N ratios in both cores are elevated during OAE2, indicating enhanced contribution of terrestrial

347   organic matter driven by a strengthened hydrologic cycle (Figure 6). In the Hope Plantation core, C/N

348   ratios increased from an average of 5.5 prior to OAE2 to 7.1 during the event, with higher values later in

349   the event, peaking around 14.4. Average values dropped back to 5.5 after OAE2, including occasional

350   peaks reflecting the inclusion of woody plant debris visible in the core. In the Smith Elementary School

351 core, C/N ratios increased from 8.4 before OAE2 to 9.53 during OAE2, with peak values (up to 16.0)

352 again occurring later in the event. Post-OAE2 C/N values at Smith Elementary are less noisy than those at
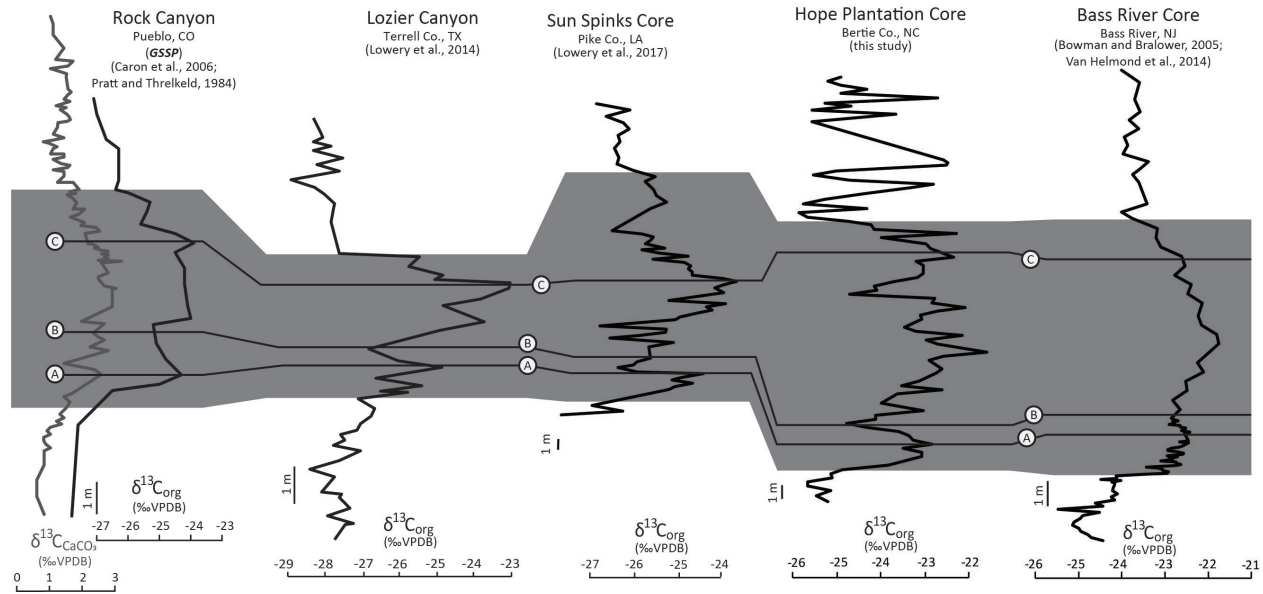
353 Hope Plantation, and average 7.4.

354

355 **Figure 7.** *Comparison of North American carbon isotope curves from the Cenomanian-Turonian GSSP at Rock*

356 *Canyon in Pueblo, CO; Lozier Canyon in Terrell Co., TX, near the transition from the Western Interior Seaway to*

357 *the Gulf of Mexico; the Sun Spinks core in Pike Co., LA on the Gulf Coastal Plain, the Hope Plantation Core from*

358 *Bertie Co., NC on the Atlantic Coastal Plain, and Bass River core from Bass River, NJ on the Atlantic Coastal*

359 *Plain. The Rock Canyon record includes both bulk carbonate (grey line) and organic carbon (black line) carbon*

360 *isotopes; all other sites only show organic carbon isotopes. The position of the A-B-C peaks are traced between the*

361 *cores. Grey bar shows the extent of OAE2 in each core.*

362 **5 Discussion**

363 **5.1 Enhanced Hydrologic Cycle During OAE2**

364   Our data indicate a strengthened hydrologic cycle in southeastern North America preceding the

365 start of OAE2 and continuing through the event, in agreement from the data from van Helmond et al.

366 (2014) some 500 km to the north. Palynological data from New Jersey agree with our bulk geochemical

367 data in showing highest terrigenous flux during the latter part of the OAE2 isotope excursion. The pre-

368 event increase in terrigenous flux is an interesting parallel to records of pre-event global oxygen

369 drawdown based on thallium isotopes (Ostrander et al., 2017), suggesting a link between weathering flux

370 and deoxygenation, likely via enhanced delivery of nutrients to the oceans. Additionally, a drop in C/N

371 ratio in both of our core records during the carbon isotope minimum referred to as the Plenus carbon

372 isotope excursion (O'Connor et al., 2020) indicate relatively drier conditions at this time, a phenomenon

373 also observed in New Jersey coincident with a decrease in temperatures (van Helmond et al., 2014). The

374 Plenus Cold Event was originally interpreted as a global cooling event (hence the name, e.g., Gale and

375 Christensen, 1996; Erbacher et al., 2005; Jarvis et al., 2011; Hasegawa et al., 2013; Gale, 2019).

376 However, more detailed comparisons of temperature and carbon isotope records from a wide range of

377 sites has demonstrated that the timing and magnitude of cooling varies significantly by location

378 (O'Connor et al., 2020). Our results agree with those of van Helmond et al. (2014) that the Plenus interval

379 resulted in a weaker hydrologic cycle and reduced terrigenous flux into the oceans, at least along the east

380 coast of North America.

381 **5.2 OAE2 on the eastern North American shelf**

382 The Smith Elementary School and Hope Plantation cores represent the second and third records

383 of OAE2 on the US Atlantic Coastal Plain. As such, they provide important insight into a surprisingly

384 understudied region. In the modern ocean, about 85% of organic carbon burial occurs along continental

385 margins (e.g., Burdige, 2007). A survey of all known OAE2 localities with a complete carbon isotope

386 excursion and TOC data by Owens et al. (2018) found that there is a significant amount of "missing"

387 organic carbon when reconstructed organic carbon burial is compared to "expected" carbon burial based

388 on carbon isotope data. This was based on 170 sites which, with some extrapolation, represent just 13%

389 of total Cenomanian–Turonian global ocean area, which meant that similar values had to be assumed for

390 the rest of the seafloor (Owens et al., 2018). OAE2 is perhaps the best studied event of the Cretaceous,

391 but these results suggest a clear need for additional sites to better constrain paleoceanographic and

392   paleoenvironmental changes during this event. By adding additional OAE2 sites on the Atlantic Coastal

393   Plain our results help to constrain the contribution of these areas to global carbon burial.

394   Van Helmond et al. (2014) point out that TOC is lower in the Bass River core than other OAE2

395   sections in the North Atlantic region, but our results indicate that Bass River is about average for inner

396   continental shelf deposits (Figure 8). Average TOC during OAE2 at Bass River is 1.1 wt% (van

397   Helmond, 2014); this is slightly higher than Smith Elementary (0.83 wt%) and Hope Plantation (0.63

398   wt%) and slightly lower than the next closest published shelf site to the southwest, the Sun Spinks core in

399   Mississippi (1.4 wt %, Lowery et al., 2017). Sequence stratigraphic analysis of Cenomanian/Turonian

400   sediments of the Clubhouse and Bass River Formations show that these sediments represent maximum

401   sea level rise across the boundary on the Atlantic Coastal Plain (Miller et al., 2004; Aleman Gonzalez et

402   al., 2020). The location of the Hope Plantation core (lowest TOC values) higher on the inner paleoshelf

403   relative to Smith Elementary School and Bass River (higher TOC values) suggests that TOC wt% on the

404   shelf during OAE2 was, at least in part, a function of paleodepth. To be sure, these TOC values are

405   certainly lower than values found offshore in the open ocean or along upwelling margins in the eastern

406   proto-North Atlantic. For example, Deep Sea Drilling Project Site 603, on the lower continental rise

407   directly offshore of North Carolina, has an average TOC of 5.4 wt % during OAE2 (Kuypers et al., 2004),

408   while the upwelling-prone region at Tarfaya, Morocco has an average TOC of 8.0 wt% (Kolonic et al.,
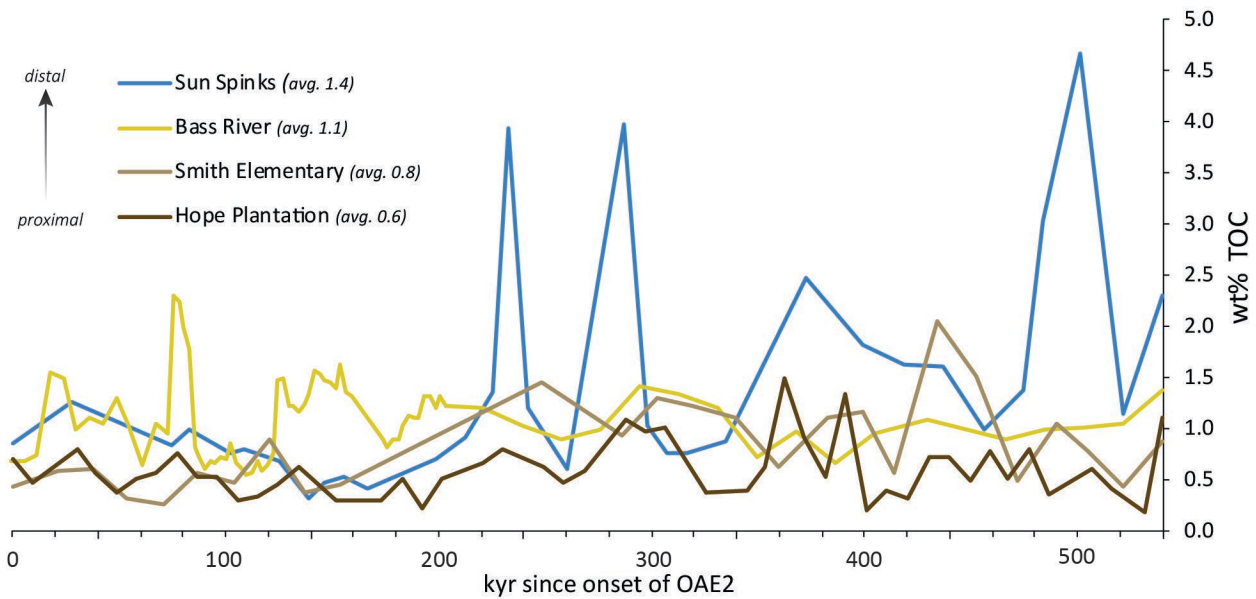
409   2005).

Figure 8. *Comparison of measured wt% TOC for the duration of OAE2 for the Sun Spinks core in Mississippi, Bass River core in New Jersey, and the Smith Elementary School and Hope Plantation cores in North Carolina. Age model based on the thickness of the OAE carbon isotope excursion and the orbitally-tuned duration of OAE2 at the Global Stratotype Section and Point in Pueblo, CO (Sageman et al., 2006; Meyers et al., 2012) of 540 kyr, assuming a constant sedimentation rate.*

Sedimentation rate also plays an important role in organic carbon accumulation. While we don't have dry bulk density measurements from these cores to calculate mass accumulation rates, we can approximate using reasonable values for organic-rich silicilastic rocks (2.4 g/cm^3, following Owens et al., 2018). We can determine the average sedimentation rate during the event using the observed thickness of the OAE2 carbon isotope excursion in each core and the orbitally-tuned duration of OAE2 at the Global Stratotype Section and Point in Pueblo, CO (Sageman et al., 2006; Meyers et al., 2012) of 540 kyr. A constant sedimentation rate on the shelf during OAE2 is almost certainly an oversimplification but it is sufficient for our purpose of comparing general trends between these cores. Using these values we find organic carbon mass accumulation rates (OC MAR) during OAE2 average 0.05 g/cm^2/kyr at Hope Plantation, 0.04 g/cm^2/kyr at Smith Elementary School, 0.06 g/cm^2/kyr at Bass River, and 0.11 g/cm^2/kyr at Spinks. For comparison, the same method indicates OC MAR rates of 0.29 g/cm^2/kyr at DSDP Site 603 and 2.84 g/cm^2/kyr at Tarfaya (Owens et al., 2018). Owens et al. (2018) found an average OC MAR on

428   shelf sites during OAE2 of 0.11 g/cm^2/kyr, which means the inner shelf sites on the east coast of North

429   America are below the global average during this event.

430   These data suggest a relationship with depth on the shelf and TOC deposition during OAE2. If

431   we arrange the sites by depth (Figure 8) we see the lowest average TOC values at Hope Plantation (0.63

432   wt%), the most proximal site; values are slightly higher at Smith Elementary (0.83 wt%) which appears to

433   represent an outer estuary or inner shelf environment, and higher still at Bass River (1.1 wt%) which was

434   inner to middle neritic (Miller et al., 2004). Estimates of organic carbon mass accumulation rates suggest

435   all three of these inner shelf sites are very similar, ranging from 0.4-0.6 g/cm^2 kyr. Average TOC is even

436   higher in the Spinks Core (1.4 wt%, or 0.11 g/cm^2 kyr), which represents inner to middle neritic depths

437   during the latter part of OAE2 (Lowery et al., 2017). This suggests the possibility of even higher values

438   on more distal parts of the shelf, and highlights the need for a true depth transect (as opposed to four cores

439   from three states) to better understand that variability and better constrain organic carbon burial in this

440   important environment during OAEs.

441   **6 Conclusions**

442   Calcareous nannoplankton biostratigraphy shows that positive carbon isotope excursions in two

443   cores on the Atlantic Coastal Plain in North Carolina are associated with the Cenomanian–Turonian

444   OAE2. C/N ratios in both cores indicate an increase in the proportion of land plants delivered to these

445   offshore sites during, indicating a strengthened hydrologic cycle causing increased terrigenous flux

446   beginning slightly before OAE2 and continuing through the whole event. This agrees with palynology-

447   based observations from the Bass River core located ~500 km to the north (van Helmond et al., 2014).

448   We therefore conclude that these changes reflect increased precipitation and weathering across eastern

449   North America during OAE2, feeding nutrients onto the shelf and into the proto-North Atlantic, and

450   likely contributing to the widespread black shale deposition in the deep basin. These cores are the second

451   and third records of OAE2, to our knowledge, on the coastal plain of eastern North America and,

452   combined with the first (Bowman and Bralower, 2005; van Helmond et al., 2014), show relatively low

453   average TOC values (~0.6 - 1.1 wt%) on the inner shelf during this event, while suggesting a trend of

454   increasing values with depth, highlighting the need for more cores in this region from middle and outer

455   shelf depths.

456   **Data Availability Statement**

457   Total organic carbon, total nitrogen, organic carbon isotope, geophysical and calcareous

458   nannofossil occurrence data are published (Self-Trail et al., 2021) and available for download as a USGS

459   Data Release at https://doi.org/10.5066/P9V0U1NF.

460   **Author Contribution**

461   CL and JS conceived of the study and sampled the cores. JS sat the wells in 2004 and 2005 and helped

462   describe the cores. CB conducted bulk organic carbon/nitrogen and organic carbon isotope measurements.

463   JS conducted calcareous nannoplankton biostratigraphy. CL supervised foraminifer analysis. CL prepared

464   the manuscript with contributions from JS and CB.

465   **Competing Interests Statement**

466   The authors declare that they have no conflicts of interest.

476 **References**

477 Aleman Gonzalez, W.B., Self-Trail, J.M., Harris, W.B., Moore, J.P., and Farrell, K.M. (2020). Depositional

478   sequence stratigraphy of Turonian to Santonian sediments, Cape Fear arch, North Carolina Coastal Plain,

479   USA. *Stratigraphy*, 17 (4), 293-314.

480 Applin, P.L., and Applin, E.R. (1944). Regional subsurface stratigraphy and structure of Florida and southern

481   Georgia. *American Association of Petroleum Geologists Bulletin, 28* (12), 1673-1753.

482 Applin, P.L., and Applin, E.R. (1947). Regional subsurface stratigraphy, structure, and correlation of middle and

483   early Upper Cretaceous rocks in Alabama, Georgia, and north Florida. *U.S. Geological Survey Oil and Gas*

484   *Investigations Chart, OC- 26*, 3 sheets.

485 Applin, P.L., and Applin, E.R., (1967). The Gulf Series in the subsurface in northern Florida and southern Georgia.

486   *U.S. Geological Survey Professional Paper 524-G*, 40 pp.

487 Arthur, M. A., Schlanger, S. T., & Jenkyns, H. C. (1987). The Cenomanian–Turonian Oceanic Anoxic Event, II.

488   Palaeoceanographic controls on organic-matter production and preservation. *Geological Society, London,*

489   *Special Publications*, *26*(1), 401-420.

490 Blättler, C. L., Jenkyns, H. C., Reynard, L. M., & Henderson, G. M. (2011). Significant increases in global

491   weathering during Oceanic Anoxic Events 1a and 2 indicated by calcium isotopes. *Earth and Planetary*

492   *Science Letters*, *309*(1-2), 77-88.

493 Bown, P.R., and Young, J.R., 1998. Techniques. In: Bown, P.R., Ed., *Calcareous Nannofossil Biostratigraphy*, 16-

494   28. London: Kluwer Academic.

495 Burdige, D. J. (2007). Preservation of organic matter in marine sediments: controls, mechanisms, and an imbalance

496   in sediment organic carbon budgets?. *Chemical reviews*, *107*(2), 467-485.

497 Burnett, J.A., 1998. Upper Cretaceous. In: Bown, P.R., Ed., *Calcareous Nannofossil Biostratigraphy*, 132-199.

498 Bowman, A. R., & Bralower, T. J. (2005). Paleoceanographic significance of high-resolution carbon isotope records

499   across the Cenomanian–Turonian boundary in the Western Interior and New Jersey coastal plain,

500   USA. *Marine Geology*, *217*(3-4), 305-321.

501 Caron, M., Dall'Agnolo, S., Accarie, H., Barrera, E., Kauffman, E. G., Amédro, F., & Robaszynski, F. (2006). High-

502   resolution stratigraphy of the Cenomanian–Turonian boundary interval at Pueblo (USA) and wadi Bahloul

503   (Tunisia): stable isotope and bio-events correlation. *Geobios*, *39*(2), 171-200.

504 Cooke, C.W. (1936). Geology of the Coastal Plain of South Carolina. *U.S. Geological Survey Bulletin 867*, 196pp.

505 Corbett, M.J., Watkins, D.K., and Pospichal, J.J., 2014. A quantitative analysis of calcareous nannofossil bioevents

506   of the Late Cretaceous (Late Cenomanian-Coniacian) Western Interior Seaway and their reliability in

507   established zonation schemes. *Marine Micropaleontology,* 109: 30-45.

508 Dorf, E., (1952). Critical analysis of Cretaceous stratigraphy and paleobotany of Atlantic Coastal Plain. *AAPG*

509   *Bulletin, 36* (11), 2161-2184.

510 Erbacher, J., Friedrich, O., Wilson, P. A., Birch, H., & Mutterlose, J. (2005). Stable organic carbon isotope

511   stratigraphy across Oceanic Anoxic Event 2 of Demerara Rise, western tropical Atlantic. *Geochemistry,*

512   *Geophysics, Geosystems*, *6*(6).

513 Friedrich, O., Norris, R. D., & Erbacher, J. (2012). Evolution of middle to Late Cretaceous oceans—a 55 my record

514   of Earth's temperature and carbon cycle. *Geology*, *40*(2), 107-110.

515 Gale, A. S., and Christensen, W. K., (1996). Occurrence of the belemnite Actinocamax plenus in the Cenomanian of

516   SE France and its significance. In *Bulletin of the Geological Society of Denmark*, *43*(1), 68-77.

517 Gale, A. (2019). Correlation, age and significance of Turonian Chalk hardgrounds in southern England and northern

518   France: The roles of tectonics, eustasy, erosion and condensation. *Cretaceous Research*, *103*, 104164.

519 Gohn, G. S. (1992). Revised nomenclature, definitions, and correlations for the Cretaceous formations in USGS-

520   Clubhouse Crossroads# 1, Dorchester County, South Carolina. *U.S. Geological Survey Professional Paper*

521   *1518*, 39 pp.

522 Gohn, G.S. 1995. Ostracode biostratigraphy of the Upper Cretaceous marine sediments in the New Jersey Coastal

523   Plain. In: Baker, J.E.B. (Ed.), Contributions to the paleontology of New Jersey. Geological Association of

524   New Jersey Annual Field Conference, 12th Annual Meeting, Wayne, NJ, Oct. 27-28, 1995, v. 12, p. 87-

525   101.Gale

526 Hasegawa, T., Crampton, J. S., Schiøler, P., Field, B., Fukushi, K., & Kakizaki, Y. (2013). Carbon isotope

527 stratigraphy and depositional oxia through Cenomanian/Turonian boundary sequences (Upper Cretaceous)

528 in New Zealand. *Cretaceous research*, *40*, 61-80.

529 Hattner, J.G., and Wise, S.W., Jr., (1980). Upper Cretaceous calcareous nannofossil biostratigraphy of South

530 Carolina. *South Carolina Geology, 24*(2), 41-117.

531 Hazel, J.E., Bybell, L.M., Christopher, R.A., Frederiksen, N.O., May, F.E., McLean, D.M., Poore, R.Z., Smith,

532 C.C., Sohl, N.F., Valentine, P.C., and Witmer, R.J., (1977). Biostratigraphy of the deep corehole

533 (Clubhouse Crossroads corehole 1) near Charleston, South Carolina, in Rankin, D.W., (Ed.), Studies related

534 to the Charleston, South Carolina earthquake of 1886—A preliminary report. *U.S. Geological Survey*

535 *Professional Paper 1028*, p. 71-89.

536 Heron, S.D., Jr. (1958). History of terminology and correlations of the basal Cretaceous formations of the

537 Carolinas. *South Carolina Division of Geology Bulletin 2*, p. 77-88.

538 Jarvis, I., Lignum, J. S., Gröcke, D. R., Jenkyns, H. C., & Pearce, M. A. (2011). Black shale deposition, atmospheric

539 CO2 drawdown, and cooling during the Cenomanian-Turonian Oceanic Anoxic

540 Event. *Paleoceanography*, *26*(3).

541 Jenkyns, H. C. (2010). Geochemistry of oceanic anoxic events. *Geochemistry, Geophysics, Geosystems*, *11*(3).

542 Kennedy, W. J., Walaszczyk, I., & Cobban, W. A. (2005). The global boundary stratotype section and point for the

543 base of the Turonian stage of the Cretaceous: Pueblo, Colorado, USA. Episodes*, 28*(2), 93-104.

544 Kolonic, S., Wagner, T., Forster, A., Sinninghe Damsté, J. S., Walsworth-Bell, B., Erba, E., Turgeon, S., Brumsack,

545 H.J., Chellai, E.H., Tsikos, H., & Kuhnt, W. (2005). Black shale deposition on the northwest African Shelf

546 during the Cenomanian/Turonian oceanic anoxic event: Climate coupling and global organic carbon

547 burial. *Paleoceanography*, *20*(1).

548 Kuypers, M. M., Lourens, L. J., Rijpstra, W. I. C., Pancost, R. D., Nijenhuis, I. A., & Damsté, J. S. S. (2004).

549 Orbital forcing of organic carbon burial in the proto-North Atlantic during oceanic anoxic event 2. *Earth*

550 *and Planetary Science Letters*, *228*(3-4), 465-482.

551   Leckie, R. M., Yuretich, R. F., West, O. L., Finkelstein, D., & Schmidt, M. (1998). Paleoceanography of the

552   southwestern Western Interior Sea during the time of the Cenomanian–Turonian boundary (Late

553   Cretaceous).

554   Leckie, R. M., Bralower, T. J., & Cashman, R. (2002). Oceanic anoxic events and plankton evolution: Biotic

555   response to tectonic forcing during the mid-Cretaceous. *Paleoceanography*, *17*(3), 13-1.

556   Lowery, C. M., Corbett, M. J., Leckie, R. M., Watkins, D., Romero, A. M., & Pramudito, A. (2014). Foraminiferal

557   and nannofossil paleoecology and paleoceanography of the Cenomanian–Turonian Eagle Ford Shale of

558   southern Texas. *Palaeogeography, Palaeoclimatology, Palaeoecology*, *413*, 49-65.

559   Lowery, C. M., Cunningham, R., Barrie, C. D., Bralower, T., & Snedden, J. W. (2017). The northern Gulf of

560   Mexico during OAE2 and the relationship between water depth and black shale

561   development. *Paleoceanography*, *32*(12), 1316-1335.

562   McAnena, A., Flögel, S., Hofmann, P. Herrle, J.O., Griesand, A., Pross, J., Talbot, H.M., Rethemeyer, J., Wallmann,

563   K., & Wagner, T., 2013. Atlantic cooling associated with a marine biotic crisis during the mid-Cretaceous

564   period. *Nature Geoscience* 6, no. 7 (2013): 558-561.

565   Meyers, P. A. (1994). Preservation of elemental and isotopic source identification of sedimentary organic matter.

566   *Chemical Geology* 114, 289-302.

567   Meyers, P. A. (1997). Organic geochemical proxies of paleoceanographic, paleolimnologic, and paleoclimatic

568   processes. *Organic geochemistry*, *27*(5-6), 213-250.

569   Meyers, P. A. (2003). Applications of organic geochemistry to paleolimnological reconstructions: a summary of

570   examples from the Laurentian Great Lakes. *Organic geochemistry*, *34*(2), 261-289.

571   Meyers, S. R., Siewert, S. E., Singer, B. S., Sageman, B. B., Condon, D. J., Obradovich, J. D., Jicha, B.R., &

572   Sawyer, D. A. (2012). Intercalibration of radioisotopic and astrochronologic time scales for the

573   Cenomanian–Turonian boundary interval, Western Interior Basin, USA. *Geology*, *40*(1), 7-10.

574   Miller, K.G., Sugarman, P.J., Browning, J.V., et al., 1998. Bass River site. *Proceedings of the Ocean Drilling*

575   *Program, Initial Reports*, v. 174AX, p. 1-39.

576   Miller, K.G., Sugarman, P.J., Browning, J.V., Kominz, M.A., Olsson, R.K., Feigenson, M.D., and Hernandez, J.C.,

577   2004. Upper Cretaceous sequences and sea-level history, New Jersey Coastal Plain. *GSA Bulletin*, 116:

578   368-393.

579   Monteiro, F. M., Pancost, R. D., Ridgwell, A., & Donnadieu, Y. (2012). Nutrients as the dominant control on the

580   spread of anoxia and euxinia across the Cenomanian-Turonian oceanic anoxic event (OAE2): Model-data

581   comparison. *Paleoceanography*, *27*(4).

582   O'Connor, L. K., Jenkyns, H. C., Robinson, S. A., Remmelzwaal, S. R., Batenburg, S. J., Parkinson, I. J., & Gale, A.

583   S. (2020). A Re-evaluation of the Plenus Cold Event, and the Links Between CO2, Temperature, and

584   Seawater Chemistry During OAE 2. *Paleoceanography and Paleoclimatology*, *35*(4), e2019PA003631.

585   Ostrander, C. M., Owens, J. D., & Nielsen, S. G. (2017). Constraining the rate of oceanic deoxygenation leading up

586   to a Cretaceous Oceanic Anoxic Event (OAE-2:~ 94 Ma). *Science advances*, *3*(8), e1701020.

587   Owens, J. D., Lyons, T. W., Hardisty, D. S., Lowery, C. M., Lu, Z., Lee, B., & Jenkyns, H. C. (2017). Patterns of

588   local and global redox variability during the Cenomanian–Turonian Boundary Event (Oceanic Anoxic

589   Event 2) recorded in carbonates and shales from central Italy. *Sedimentology*, *64*(1), 168-185.

590   Owens, J. D., Lyons, T. W., & Lowery, C. M. (2018). Quantifying the missing sink for global organic carbon burial

591   during a Cretaceous oceanic anoxic event. *Earth and Planetary Science Letters*, *499*, 83-94.

592   Petters, S.W., 1976. Upper Cretaceous subsurface stratigraphy of Atlantic Coastal Plain of New Jersey. *AAPG*

593   *Bulletin*, v. 60, n. 1, p. 87-107.

594   Petters, S.W., 1977. Upper Cretaceous planktonic foraminifera from the subsurface of the Atlantic Coastal Plain of

595   New Jersey. *Journal of Foraminiferal Research*, 7: 165-187.

596   Pogge Von Strandmann, P. A., Jenkyns, H. C., & Woodfine, R. G. (2013). Lithium isotope evidence for enhanced

597   weathering during Oceanic Anoxic Event 2. *Nature Geoscience*, *6*(8), 668-672.Prahl et al., 1980

598   Pratt, L. M., & Threlkeld, C. N. (1984). Stratigraphic significance of 13C/12C ratios in mid-Cretaceous rocks of the

599   Western Interior, USA.

600 Richards, H.G. (1945). Subsurface stratigraphy of Atlantic Coastal Plain between New Jersey and Georgia.

601 *American Association of Petroleum Geologists Bulletin, 29* (7), 885-955.

602 Sageman, B. B., Meyers, S. R., & Arthur, M. A. (2006). Orbital time scale and new C-isotope record for

603 Cenomanian–Turonian boundary stratotype. *Geology*, *34*(2), 125-128.

604 Schlanger, S. O., & Jenkyns, H. C. (1976). Cretaceous oceanic anoxic events: causes and consequences. *Geologie en*

605 *mijnbouw*, *55*(3-4).

606 Scholle, P. A., & Arthur, M. A. (1980). Carbon isotope fluctuations in Cretaceous pelagic limestones: potential

607 stratigraphic and petroleum exploration tool. *AAPG Bulletin*, *64*(1), 67-87.

608 Seefelt, E.L., Self-Trail, J.M., and Schultz, A.P., 2015. Comparison of three preservation techniques for slowing

609 dissolution of calcareous nannofossils in organic-rich sediments. *Micropaleontology*, v. 61, n. 3, p. 149-

610 164.

611 Self-Trail, J.M., and Bybell, L.M., 1995. Cretaceous and Paleogene calcareous nannofossil biostratigraphy of New

612 Jersey. In: Baker, J.E.B. (Ed.), Contributions to the paleontology of New Jersey. Geological Association

613 of New Jersey Annual Field Conference, 12th Annual Meeting, Wayne, NJ, Oct. 27-28, 1995, v. 12, p. 102-

614 139.

615 Self-Trail, J.M., and Seefelt, E.L., 2005. Rapid dissolution of calcareous nannofossils: a case study from freshly

616 cored sediments of the south-eastern Atlantic Coastal Plain. *Journal of Nannoplankton Research*, v. 27, n.

617 20, p. 149-157.

618 Self-Trail, J.M., Barrie, C., and Lowery, C.M., 2021. Isotope, organic carbon, and biostratigraphic data for the Hope

619 Plantation (BE-110) and Smith Elementary School (CR-675) cores, North Carolina. USGS Data Release.

620 https://doi.org/10.5066/P9V0U1NF.

621 Shamrock, J.L., Munoz, E.J., and Carter, J.H., 2015. An improved sample preparation technique for calcareous

622 nannofossils in organic-rich mudstones. *Journal of Nannoplankton Research*, v. 35, n. 2, 101-110.

623 Shamrock, J.L., and Self-Trail, J.M., 2016. Quantification of a pretreatment procedure for organic-rich calcareous

624 nannofossil samples. *Journal of Nannoplankton Research*, v. 36, n. 1, 65-75.

625   Sikora, P.J., and Olsson, R.K., 1991. A paleoslope model of late Albian to early Turonian foraminifera of the

626   western Atlantic margin and North Atlantic basin. Marine Micropaleontology, v. 18, p. 25-72.

627   Sissinghi, W., 1977. Biostratigraphy of Cretaceous calcareous nano;lankton. *Geologie en Mijnbouw*, 56: 37-65.

628   Slattery, J. S., Cobban, W. A., McKinney, K. C., Harries, P. J., & Sandness, A. L. (2015). Early Cretaceous to

629   Paleocene paleogeography of the Western Interior Seaway: the interaction of eustasy and

630   tectonism. *Wyoming Geological Association Guidebook*, *2015*, 22-60.

631   Snedden, J. W., Virdell, J., Whiteaker, T. L., & Ganey-Curry, P. (2015). A basin-scale perspective on Cenomanian–

632   Turonian (Cretaceous) depositional systems, greater Gulf of Mexico (USA). *Interpretation*, *4*(1), SC1-

633   SC22.

634   Snow, L. J., Duncan, R. A., & Bralower, T. J. (2005). Trace element abundances in the Rock Canyon Anticline,

635   Pueblo, Colorado, marine sedimentary section and their relationship to Caribbean plateau construction and

636   oxygen anoxic event 2. *Paleoceanography*, *20*(3).

637   Spangler, W. B. (1950). Subsurface geology of Atlantic coastal plain of North Carolina. *AAPG Bulletin*, *34*(1), 100-

638   132.

639   Sohl, N. F., & Owens, J. P. (1991). Cretaceous stratigraphy of the Carolina coastal plain.*The geology of the

640   Carolinas*, 191-220.

641   Stephenson, L.W., 1912. The Cretaceous formations. In: Clark, W.B., Miller, B.L., Stephenson, L.W., Johnson,

642   B.L., and Parker, H.N., Eds. The Coastal Plain of North Carolina. *North Carolina Geologic and Economic

643   Survey*, 3: 73-171.

644   Tarduno, J. A., Sliter, W. V., Kroenke, L., Leckie, M., Mayer, H., Mahoney, J. J., Musgrave, R., Sotery, M., &

645   Winterer, E. L. (1991). Rapid formation of Ontong Java Plateau by Aptian mantle plume

646   volcanism. *Science*, *254*(5030), 399-403.

647   Thornburg, J., 2008. "Temporal variations in the paleopedology and paleoclimatology of the Early

648   Cretaceous Potomac Group, Hope Plantation core, Bertie County, North Carolina". Unpublished

649   Masters Thesis, Temple University, Pennsylvania.

650   Tibert, N. E., & Leckie, R. M. (2004). High-resolution estuarine sea level cycles from the Late Cretaceous:

651   Amplitude constraints using agglutinated foraminifera. *The Journal of Foraminiferal Research*, *34*(2), 130-

652   143.

653   Tsikos, H., Jenkyns, H. C., Walsworth-Bell, B., Petrizzo, M. R., Forster, A., Kolonic, S., ... & Damsté, J. S. (2004).

654   Carbon-isotope stratigraphy recorded by the Cenomanian–Turonian Oceanic Anoxic Event: correlation and

655   implications based on three key localities. *Journal of the Geological Society*, *161*(4), 711-719.

656   Turgeon, S. C., & Creaser, R. A. (2008). Cretaceous oceanic anoxic event 2 triggered by a massive magmatic

657   episode. *Nature*, *454*(7202), 323-326.

658   Valentine, P. C. (1982). *Upper Cretaceous subsurface stratigraphy and structure of coastal Georgia and South*

659   *Carolina*. U.S. Geological Survey Professional Paper 1222, 33 p.

660   Valentine, P.C., (1984). Turonian (Eaglefordian) stratigraphy of the Atlantic Coastal Plain and Texas. *U.S.*

661   *Geological Survey Professional Paper 1315*, 21pp.

662   van Helmond, N. A., Sluijs, A., Reichart, G. J., Damsté, J. S. S., Slomp, C. P., & Brinkhuis, H. (2014). A perturbed

663   hydrological cycle during Oceanic Anoxic Event 2. *Geology*, *42*(2), 123-126.\

664   van Helmond, N. A., Sluijs, A., Sinninghe Damsté, J. S., Reichart, G. J., Voigt, S., Erbacher, J., ... & Brinkhuis, H.

665   (2015). Freshwater discharge controlled deposition of Cenomanian–Turonian black shales on the NW

666   European epicontinental shelf (Wunstorf, northern Germany). *Climate of the Past*, *11*, 495-508.

667   Weems, R. E., Seefelt, E. L., Wrege, B. M., Self-Trail, J. M., Prowell, D. C., Durand, C., Cobbs, E.F., & McKinney,

668   K. C. (2007). Preliminary physical stratigraphy and geophysical data of the USGS Hope Plantation Core

669   (BE-110), Bertie County, North Carolina. *US Geological Survey Open-File Report*, *1251*, 1-163.

670   Weems, R. E., Self-Trail, J. M., and Edwards, L. E., 2019. Cross Section of the North Carolina Coastal Plain from

671   Enfield through Cape Hatteras. *US Geological Survey Open-File Report,* 2019-1145.

672   Whitechurch, H., Montigny, R., Sevigny, J., Storey, M., & Salters, V. (1992). K-Ar and 40Ar-39Ar ages of central

673   Kerguelen Plateau basalts. In *Proc. Ocean Drill. Program Sci. Results* (Vol. 120, pp. 71-77).

674   Zarra, L. (1989). *Sequence stratigraphy and foraminiferal biostratigraphy for selected wells in the Albemarle*

675   *Embayment, North Carolina*. North Carolina Geological Survey Open File Report 89-5. 52 p.